PHILOSOPHICAL TRANSACTIONS OF THE ROYAL SOCIETY B BIOLOGICAL SCIENCES

Three-Dimensional Reconstruction of the Stacked-Disk Aggregate of Tobacco Mosaic Virus Protein from Electron Micrographs

J. T. Finch and A. Klug

Phil. Trans. R. Soc. Lond. B 1971 **261**, 211-219
doi: 10.1098/rstb.1971.0053

Phil. Trans. Roy. Soc. Lond. B. **261**, 211–219 (1971) [211]
Printed in Great Britain

Three-dimensional reconstruction of the stacked-disk aggregate of tobacco mosaic virus protein from electron micrographs

By J. T. Finch and A. Klug, F.R.S.
Medical Research Council, Laboratory of Molecular Biology, Hills Road, Cambridge

[Plate 42]

The three-dimensional structure of the stacked-disk rod of tobacco mosaic virus protein has been reconstructed to a resolution of about 2 nm from electron microscope images. Closed rings of seventeen protein subunits (compared with $16\frac{1}{3}$ in one turn of the virus helix) are stacked in polar fashion, the stacking being accompanied by an axial perturbation of periodicity 5.3 nm connecting successive pairs of rings into disks. The axial perturbation consists of a movement towards each other of the outer parts of the subunits in the two rings comprising a disk, together with a movement of the inner parts in the opposite direction. This could be explained either by a bending of parts of the subunits in the appropriate directions or by a bodily tilting of the subunits in the two rings in opposite directions.

Introduction

The three-dimensional reconstruction method of DeRosier & Klug (1968) has been applied to electron micrographs of the 'stacked-disk' rod-shaped aggregate of the protein of tobacco mosaic virus (see, for example, Klug & Caspar 1960). Stacked-disk rods are built from rings of seventeen protein subunits (Finch, Leberman, Chang & Klug 1966) the rings being associated in pairs ('disks') along the length of the particle. Free two-ring disks are also found and these appear to be stable intermediates in the formation of stacked-disk rods. A rod-like structure built of stacked rings could well arise as a simple variant of the helical structure of the intact virus particles, i.e. one in which the protein subunits have a similar bonding pattern to that in the virus, but—in the absence of the RNA–protein interaction—with small local differences leading to a rotational rather than helical symmetry. Thus the number of subunits per ring, 17, is close to the number of subunits per turn of the virus helix, $16\frac{1}{3}$, so that the lateral bonding between subunits is clearly very similar in the two structures. The existence of pairing between rings shows, however, that the variation is not a trivial one, and the unknown factor is the relationship between the two rings comprising a disk.

If the stacked-disk structure were a simple variant of the helical structure then successive rings should face in the same direction as do the successive turns of the helix, i.e. the structure is polar. However, polar aggregation of rings would be expected to continue indefinitely and not stop at the two-ring stage unless there is an additional axial perturbation between pairs of rings, as suggested by Caspar (1963, see also Caspar & Holmes 1969). But an alternative and far simpler explanation of the pairing between rings would be that they face in opposite ways and are thus related by twofold axes perpendicular to the axis of the rings. The bonding between rings would then be unrelated to that between turns of the virus helix. The purpose of this investigation was to see whether there was enough information in the electron micrographs to distinguish between these two possibilities.

In the course of this work, we have discovered a new polymorphic form of TMV protein, the double helical structure. This has turned out to be, as described below, a helical variant of the stacked-disk structure in which the two rings of a disk become, by a small change in the angle of bonding, the successive turns of a flat, two-start helix.

Selection of the images

In the first instance, electron micrographs of negatively stained, stacked-disk rods were scanned by eye in order to find particle images which were straight, apparently undistorted and uniformly stained over a length of at least ten disks. (A very common distortion is flattening, but the more severe cases can easily be detected by measurements of the diameter.) These images were then examined by optical diffraction directly from the electron microscope plates, and those giving clear optical transforms with symmetrical layer-lines were selected for further investigation. The optical transform records only the amplitudes of the diffracted intensity, and a much better indication of the state of preservation of the particle symmetry is given by an examination of the phases of the diffraction pattern. These phases can be generated by computing the Fourier transform of a digitized image (DeRosier & Klug 1968). The correlation of the phases on the left and right sides of each layer-line in the transform is a measure of the degree of preservation of the helical symmetry in the stained particles.

However, in order to be able to compare phases directly, it is necessary that the origin used in the computations lie exactly on the axis of the particle. The axis can be located accurately by comparing the phases of the maxima of amplitude on the two opposite sides of a layer-line. The procedure is, therefore, first to make a visual estimate of the position of the axis of the particle—in practice we have found that this can be done to an accuracy of about 0.3 nm—and then calculate the Fourier transform with respect to a point on this axis as origin. Graphs of the amplitudes and phases along a prominent layer-line of a stacked-disk transform for a phase origin chosen visually are shown in figure 1*a*. The structure factor along this layer-line involves the zero-order Bessel function J_0, and for this and all other layer-lines involving only even order Bessel functions, the amplitudes and phases of corresponding maxima on opposite sides of the layer-line should be equal for a particle with perfect helical symmetry. (For layer-lines involving Bessel functions of odd order, i.e. arising from helical families with an odd number of members, the phases of corresponding peaks on the left and right sides of the layer-lines will differ by 180°.) In the case of figure 1*a* the phase angles of peaks on the left side are consistently lower than the phases of their counterparts on the right by an amount $\delta\phi$ proportional to R, the reciprocal spacing along a layer-line measured from the meridional line. The phase origin in the image must therefore be shifted to the right through a distance $\delta\phi/(2 \times 360°) \times 1/R$ in order to equalize phases of corresponding peaks: this has been done to produce figure 1*b*. In this way, the particle axis can be located to within about 0.025 nm in favourable cases. This procedure must be modified when the particle axis is not perpendicular to the electron beam (DeRosier & Moore 1970). In the case of images where it was not possible to correct the phase origin consistently in this way for all peaks on all layer-lines, the particle in question was considered to be so distorted or unevenly stained as not to be worth processing any further.

The best particles thus selected contained significant detail to spacings of about 1.7 nm.

Cylindrically averaged structure

One of the best images of a stacked-disk rod, selected as described above is shown in figure 2, plate 42. Its Fourier transform, calculated and displayed according to the procedures of DeRosier & Moore (1970), is shown in figure 4 *a* and *b*. The layer-line at $Z = 0.4\ \mathrm{nm}^{-1}$ corresponds to the axial spacing of 2.5 nm between rings; that at $Z = 0.2\ \mathrm{nm}^{-1}$ corresponds to the 5 nm spacing†

† The particles which we believe to be the best preserved have an inter-disk spacing closer to 5.3 nm, but it is convenient to use the round figure.

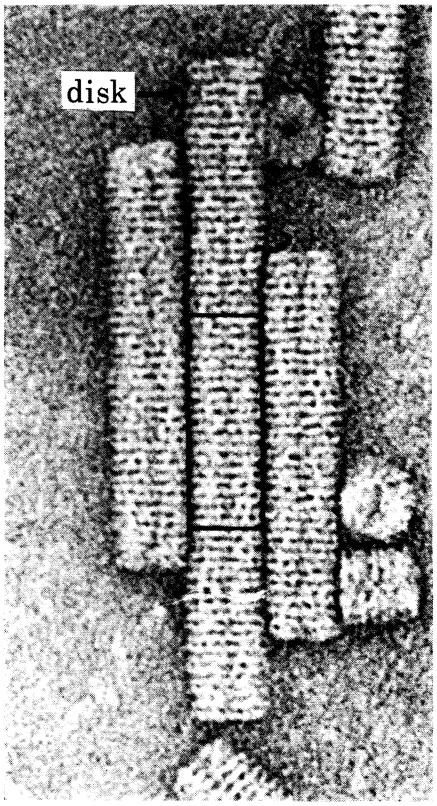

2

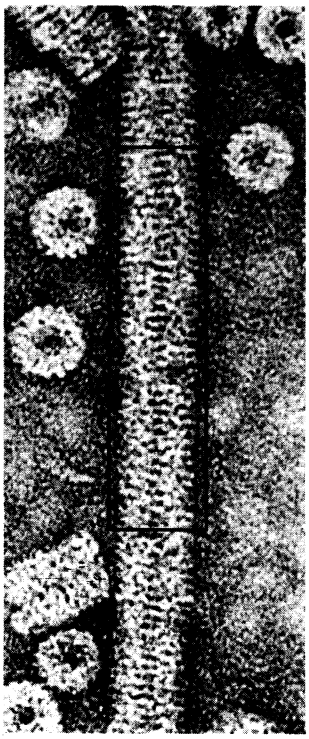

3

FIGURE 2. Electron micrograph of stacked-disk rods of tobacco mosaic virus protein, negatively stained with uranyl acetate (magn. × 550 000).

FIGURE 3. The double-helical aggregate of TMV protein, negatively stained with uranyl acetate (magn. × 550 000).

(*Facing p.* 212)

PHILOSOPHICAL TRANSACTIONS OF THE ROYAL SOCIETY B BIOLOGICAL SCIENCES

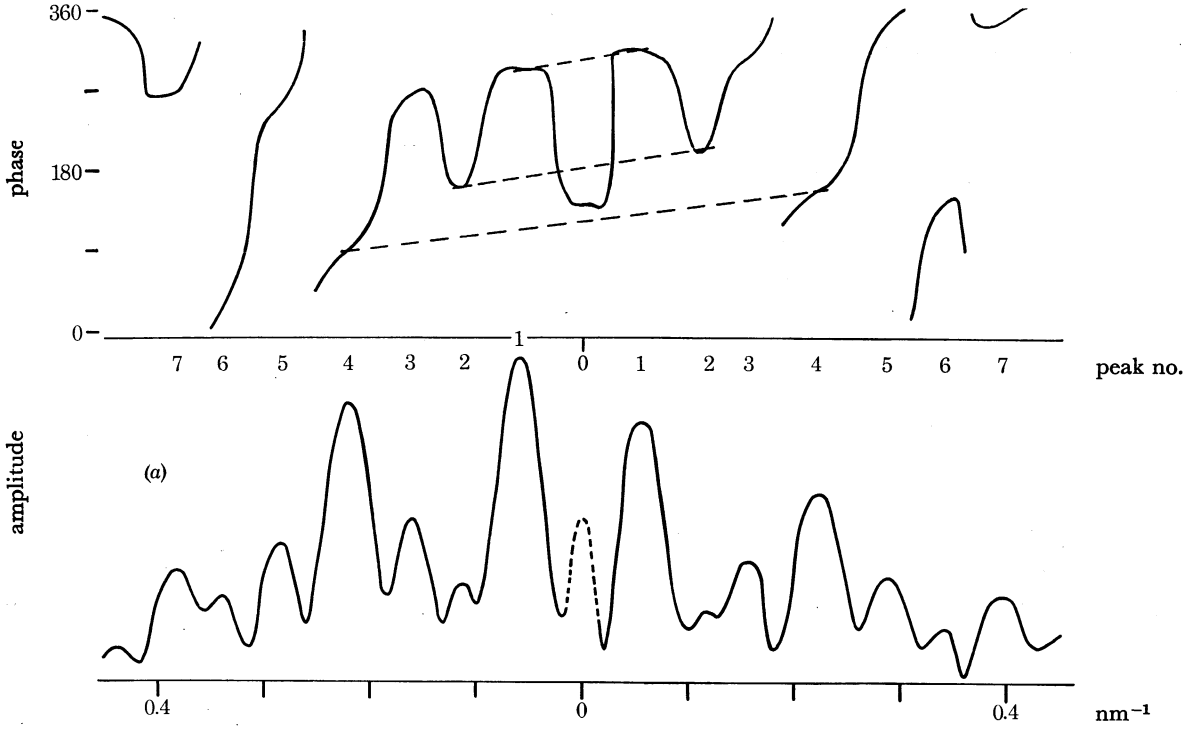

(*a*) Variation of the amplitude and phase of the structure factor of a stacked-disk rod along the layer-line at 0.2 nm^{-1}, calculated for an origin located on the axis, the lateral position of the axis being estimated visually. Peaks in the amplitude are numbered to the left and right starting from the meridian. There is an obvious difference in phase angle between corresponding peaks on the left and right sides. The magnitude of the difference is proportional to the distance of the peak from the meridian, as illustrated by the constancy of slope of the dotted lines joining the phases of peaks 1, 2, and 4 on the two sides.

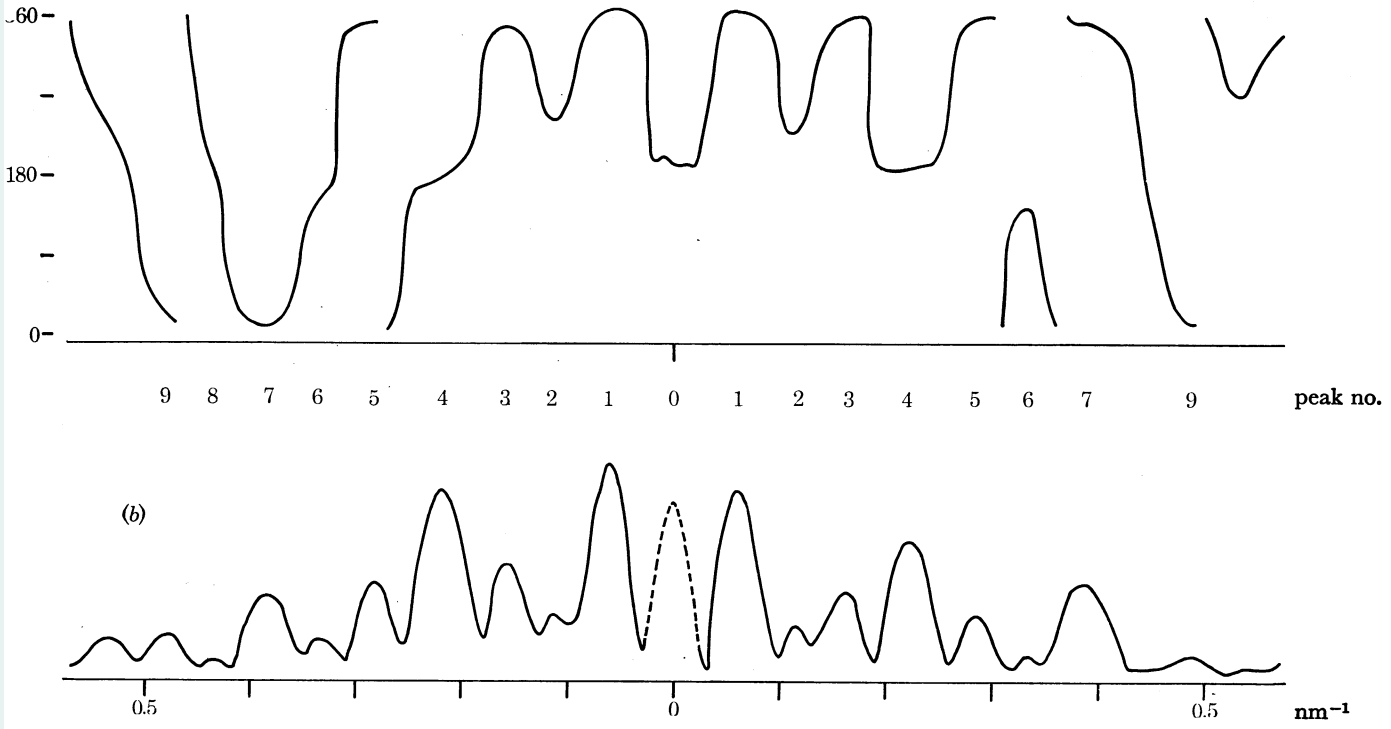

(*b*) Structure-factor recalculated after correction of the position of the axis. The shift involved was 0.4 nm. The phase angles on the left and right sides agree well, and the phase correlation can be extended as far as peak 9. (The small differences in amplitude compared with (*a*) are due to a slight change in the choice of boundaries of the region from which the transform was calculated.)

FIGURE 1. Location of axis of a helical particle by use of phase correlation.

PHILOSOPHICAL TRANSACTIONS OF THE ROYAL SOCIETY B BIOLOGICAL SCIENCES

between disks and its strength is a measure of the difference between successive rings, i.e. of the pairing association within a disk. These two layer-lines contain contributions of the type

$$J_0(2\pi Rr)\exp(2\pi iZz)$$

and give information on the radial (r) and longitudinal variations (z) in the density. Considered in isolation from the rest of the diffraction pattern, they correspond to a cylindrical projection

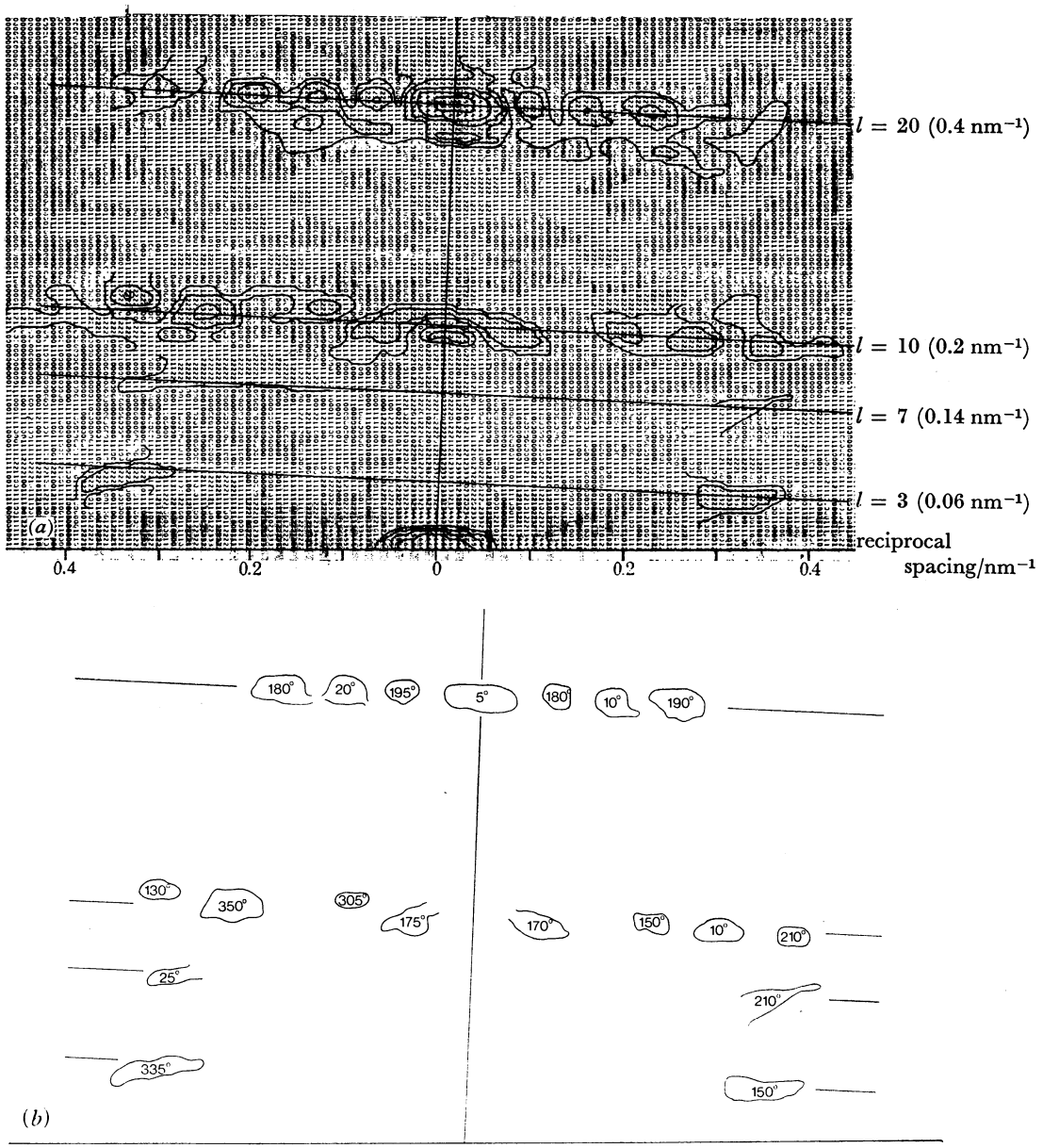

FIGURE 4. (a) A map of the amplitudes of the Fourier transform of the section of the image shown boxed in figure 2. The amplitude peaks occur on the layer-lines marked and are shown contoured. The helical selection rule for the diffraction pattern is $n = 17n'$ where n' is given by $l = 3n' + 10m$. (b) A tracing of the peak contours in (a) with the values of the phase angle (in degrees) which have been read off from the computed phase output. Layer-lines $l = 10$ and 20 arise from the cylindrically averaged structure and the phases of corresponding peaks on the left and right sides should ideally be the same. Layer-lines 3 and 7 arise from azimuthal variations in the density, i.e. from families of 17 parallel helices running through the subunits of each disk. Because this rotational symmetry is of odd order, the phases of corresponding peaks on the left and right of layer-lines should ideally differ by 180°.

PHILOSOPHICAL TRANSACTIONS OF THE ROYAL SOCIETY B BIOLOGICAL SCIENCES

of the three-dimensional structure on to a plane containing the axis (Klug, Crick & Wyckoff 1958). This projection is independent of the state of order of the relative azimuthal or rotational disposition of disks, and since most particles showed evidence of azimuthal disorder (as judged by the absence of other clear layer-lines in the diffraction patterns), it was decided to concentrate on the cylindrically averaged structure as a first approach.

From the values of the transform along the 0.2 and 0.4 nm^{-1} layer-lines, therefore, a section of the cylindrically averaged structure was computed for each image and a typical example is shown in figure 5.† There are variations in detail in the maps computed from different micrographs but all show main features in common. In each case the subunits of the two rings within a disk are bunched together at the outside of the particle (over a range of radius of 8 to 9 nm), and, at inner radii (2 to 4 nm), adjacent rings belonging to neighbouring disks appear to be even more strongly bunched together. A region of low density occurs at a radius of about 4 nm, presumably corresponding to the hole left in the structure by the absence of RNA, which is located at that radius in the intact virus.

The cylindrically averaged structure at the low resolution with which the map was calculated shows a strong tendency towards mirror symmetry about a radial line through the centre of a disk—this mirroring would follow naturally if a disk were composed of rings face-to-face. However, a polar, cylindrical variant of the normal helical structure could well also present a mirrored appearance at low enough resolution, in so far as protein molecules, or parts of them, are not distinguishable from ellipsoids, and the axes of the ellipsoids are not tilted appreciably from the radial direction. Some particles do have stronger polar features than that which gave figure 5, but is hard to evaluate the relative reliability of different maps.

A DOUBLE-HELICAL VARIANT

During this study, certain images were identified by optical diffraction as deriving from a variant of the stacked-disk structure in which the subunits are arranged in a double-helical array. A similar variant has been found in the case of barley stripe mosaic virus (Kiselev, DeRosier & Atabekov 1969). One such image is shown in figure 3, plate 42. The diameter of these images is again similar to that of the virus particles, and adjacent turns are associated in pairs in a similar fashion to the way in which adjacent rings of the stacked-disk structure are paired. The Fourier transform again shows layer-lines corresponding to spacings of about 5 and 2.5 nm, but these now contain off-meridional maxima which can be identified as contributions from the Bessel functions J_1 and J_2 respectively, rather than from J_0. From the data on these layer-lines, a projection of the structure in the basic helical direction onto an axial plane was calculated (figure 6). This 'helical' projection (Klug *et al.* 1958) is the exact counterpart of the cylindrical projection for the stacked-disk structure. The map shows features very similar to those of the cylindrically-averaged stacked-disk structure, notably the bunching of matter to give a 5 nm modulation in the axial direction at both inner and outer radii. There is a small degree of polarity in the map, indicating that the two helical arrays in the structure are parallel

† The equator was routinely omitted from the final Fourier computations, since it is extremely sensitive to departures from cylindrical symmetry in the stain distribution, which do not, however, affect other layer-lines. The maps therefore have both positive and negative densities. The effect of the omission of the equator is that the average density at each radius is zero, i.e. densities at different radii are not plotted at the correct levels, but at any one particular radius, the variations of density in the longitudinal and azimuthal directions are unaffected.

PHILOSOPHICAL TRANSACTIONS OF THE ROYAL SOCIETY B BIOLOGICAL SCIENCES

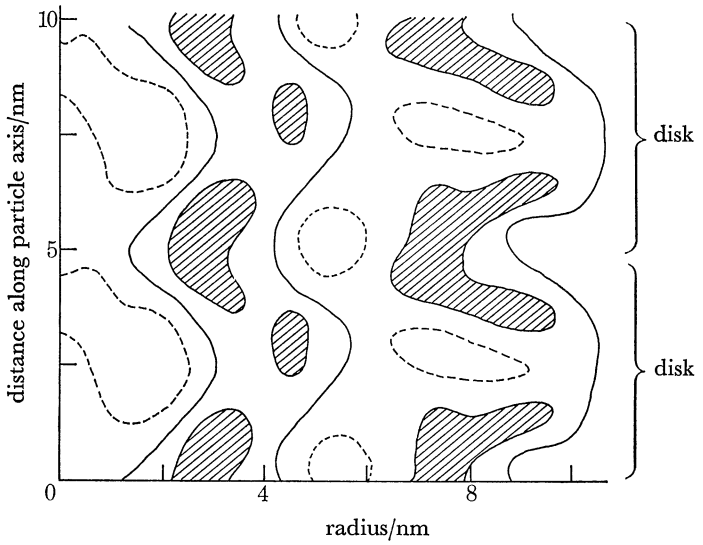

FIGURE 5. A section through the particle axis of the cylindrically averaged structure of a stacked-disk rod. It was computed from the data on the layer-lines $l = 10$ and 20 of the Fourier transform of an electron microscope image (see figure 4). Since the equatorial data was not included, the map shows both positive and negative density. The full contour shows the zero level, positive density peaks are shaded and strong negative densities (holes) are shown by the broken contour lines. The subunits of adjacent rings are bunched together at radii of 8 to 9 nm within disks and at radii 2 to 4 nm between disks. From the nature of the Fourier–Bessel synthesis, errors in the computed density tend to accumulate near the axis of the structure, but the actual weight involved is negligible at these small radii.

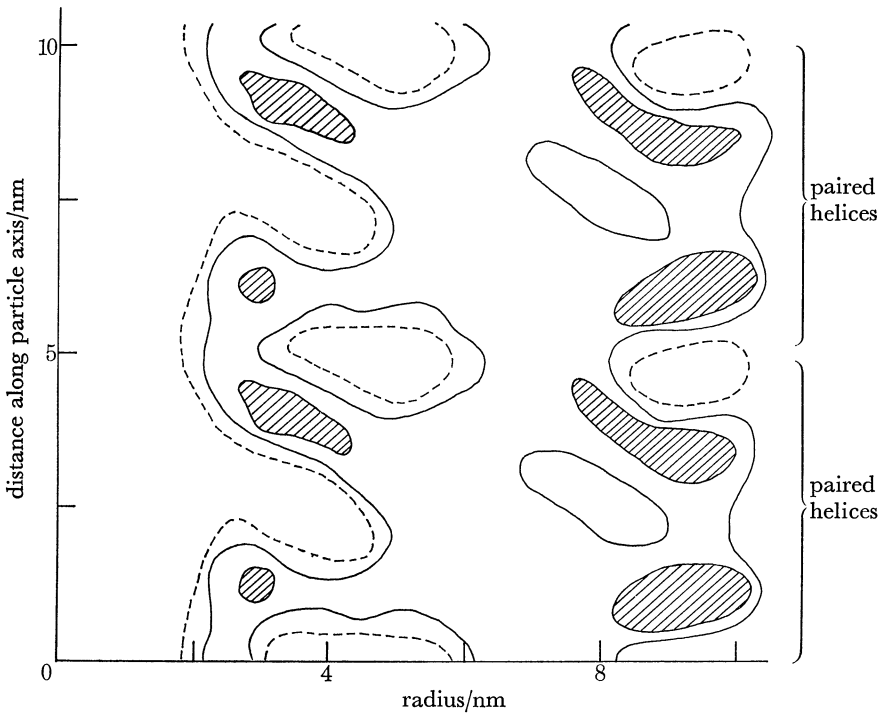

FIGURE 6. A section through the particle axis of the projection of a double-helix rod down the basic helix. This helical projection is the exact analogue of the cylindrical projection shown in figure 5, since the double-helical structure is a variant of the stacked-disk structure in which pairs of adjacent rings of subunits have become paired helical lines of subunits. The main features in this map are very similar to those in figure 5.

rather than antiparallel. However, the deviations from mirror symmetry which indicate the absence of dyads perpendicular to the helix axis are not large, so that the results from this projection must be treated with as much caution as those in the last section.

Full three-dimensional reconstruction

The cylindrical projection of the stacked-disk rod, although clearly showing the pairing of the subunits in adjacent rings, is only marginally adequate, at a resolution of about 2 nm, to distinguish between polar and non-polar structures. The reconstruction method was, therefore, further applied in three dimensions in order to obtain a more complete picture of the disposition

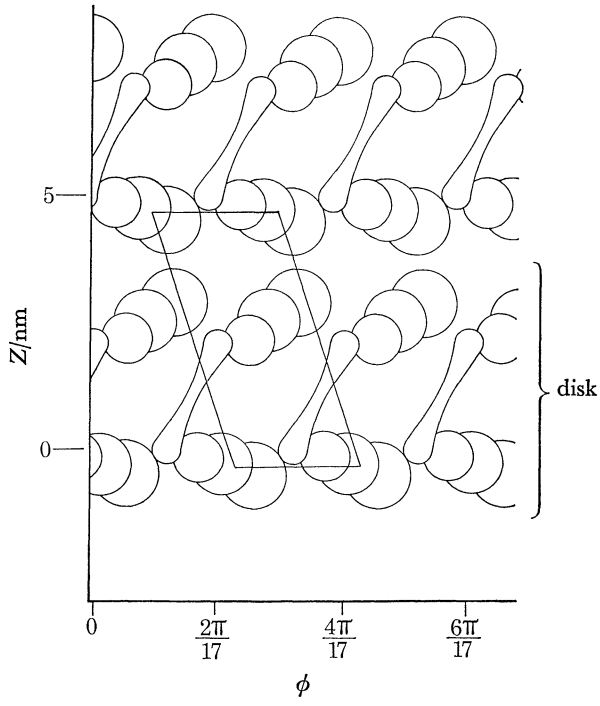

Figure 7. The surface structure of the stacked-disk rod.

Cylindrical sections of the three-dimensional reconstruction of a stacked-disk rod are shown superposed in radial projection. The sections are at radii 10, 9, 8 and 7 nm. The contour levels were chosen to show the main positive density peaks on each section and hence locate the main body of the protein subunits at each radius. This reconstruction is the average of those from three 'best' particle images. The individual reconstructions all show the same features indicative of a polar structure, namely, all the subunits slew azimuthally in the same direction and those in adjacent rings are not tilted from the horizontal to the same extent. The parallelogram marks the boundaries of a unit cell containing two non-crystallographically equivalent subunits. The rotational stagger between a ring and the next-but-one ring 5.3 nm apart is almost identical to that between two turns in the virus helix which are two pitch distances (4.6 nm) apart. The surface lattices of the two structures are therefore similar in their geometry.

of individual subunits. This involved searching many more images to find particles in which the azimuthal order between disks was maintained over long enough stretches—at least two axial repeats. The layer-lines at 0.06 and 0.14 nm^{-1} in the Fourier transform (figure 1) reflect the azimuthal ordering between disks. From the positions of these layer-lines, the screw angle between successive disks can be found. It is $\frac{3}{10}$ of $2\pi/17$, leading to an axial repeat of 10×5 nm $= 50$ nm. The two layer-lines correspond to the third and seventh orders of this period. By including the data from these layer-lines in the Fourier–Bessel synthesis, the complete

three-dimensional structure of the stacked-disk rod can be computed including the azimuthal density variations. This has been done for the three best images we found. The criterion used in searching for these particles was the clarity of the 0.06 and 0.14 nm^{-1} layer-lines, which indicates that the long-range azimuthal order between disks was reasonably well preserved. This was finally checked by the relatively good correlation between the phases on the left and right sides of each layer-line.

It was also notable that these best particles, selected according to internal criteria only, had transforms which agreed well with the low-angle part of the X-ray patterns obtained from oriented gels of stacked-disk rods (J. T. Finch, unpublished). Thus the structure deduced from the Fourier analysis of the electron micrographs has the correct helical parameters and repeat distance. The three-dimensional model constructed from these data may thus reasonably be expected to be valid for the structure of the rods in solution.

Cylindrical sections of the density, i.e. two-dimensional maps on a series of coaxial cylindrical surfaces at fixed radial intervals, were calculated and the high density regions contoured to locate the main body of the subunits at each radius. The purpose of using this form of grid for the Fourier–Bessel synthesis is that the disposition of the subunits can be easily seen by superposing the cylindrical sections in order of their radius. The reconstructions from the three particles chosen show reasonable agreement and can be themselves superposed on each other fairly closely. The result of averaging the maps of the three particles is shown in figure 7 (see footnote on p. 215). The pairing of the subunits in the axial direction at large radii is again evident, but it is also seen that subunits in alternate rings are not tilted from the horizontal to exactly the same extent. Furthermore, the subunits in both the rings comprising a disk slew in the *same* direction, i.e. the azimuth of the centre of the mass of the subunit varies with increasing radius in the same way for each of the two rings. Both of these features are inconsistent with a disk built from two rings face-to-face and related by a twofold axis. Although the deviation from twofold symmetry is not a dominant feature of the structure at this low resolution, the fact that it is present to about the same extent for all three particles—and these are the 'best' particles found—does strongly indicate a polar structure.

Conclusions

The results strongly suggest that the bonding in the stacked-disk structure is a variant of that in the normal virus helix: the disks are polar structures and the pairing of the rings within a disk appears to be associated with a movement of the outer parts of the subunits towards each other in an axial direction, as shown in figure 7. This pairing gives rise to the modulation or perturbation of periodicity 5 nm in the axial direction located in the radial range 8 to 9.5 nm. The inner parts of the subunits in the radial range 2 to 4 nm appear to move in the opposite direction, to produce a bunching in the contact region between disks (figure 5). Presumably this bunching is associated with the interaction between disks which leads to their stacking into rods. This interaction is known to be very strong, in so far as stacked-disk rods, once formed, are not easily dissociated again (A. C. H. Durham, unpublished results).

The movements described above which connect rings of subunits into pairs may be accounted for in two ways, which cannot be distinguished at the resolution of the present investigation:

(*a*) The outer ends of subunits in the two rings bend towards each other and the inner ends away from each other. This perturbation from a simple arrangement of rings stacked in polar fashion might be described as a 'pairing distortion'.

PHILOSOPHICAL TRANSACTIONS OF THE ROYAL SOCIETY B BIOLOGICAL SCIENCES

(*b*) Alternatively there is a bodily tilting of the subunits in the two rings in opposite directions. This would result in the ends of the subunits moving in the same way as in (*a*), but without the necessity for invoking large movements of different parts of a subunit relative to one another. Although tilting is the most simple explanation, the possibility of an accompanying distortion is by no means implausible in view of the observations of Caspar & Holmes (1969) on the Dahlemense strain of the virus. Here a deformation of a bending type must be postulated in order to account for movements of up to 0.4 nm in the positions of the outer ends of the subunits.

The conclusion that the stacked-disk structure is a (polar) variant of the helical structure is consistent with X-ray diffraction photographs which have recently been obtained from oriented gels of the stacked-disk rods (J. T. Finch, unpublished work). The distribution of regions of strong intensity in these X-ray diagrams as far out as the 0.8 nm region is very similar to that in the X-ray diagrams of protein polymerized into the single (virus-like) helix (Franklin 1955). This resemblance is not surprising since the angular relation between adjacent disks 5.3 nm apart is close to that between turns of the single helix which are two pitch distances (4.6 nm) apart. The fact that the long-range geometry of the packing of subunits is only slightly different in the two structures would by itself speak for a close relation between the bonding in the stacked-disk and helical forms.

We thank Dr R. Leberman for supplying preparations of reaggregated TMV protein. Various forms of the computer programs, finally embodied in the system of DeRosier & Moore (1970), were developed by Dr DeRosier during the course of the analysis described here, and we thank him for his help.

References (Finch & Klug)

Caspar, D. L. D. 1963 *Adv. Protein Chem.* **18**, 37.
Caspar, D. L. D. & Holmes, K. C. 1969 *J. molec. Biol.* **46**, 99.
DeRosier, D. J. & Klug, A. 1968 *Nature, Lond.* **217**, 130.
DeRosier, D. J. & Moore, P. B. 1970 *J. molec. Biol.* **52**, 355.
Finch, J. T., Leberman, R., Chang, Y. & Klug, A. 1966 *Nature, Lond.* **212**, 349.
Franklin, R. E. 1955 *Biochim biophys. Acta* **18**, 313.
Kiselev, N. A., DeRosier, D. J. & Atabekov, J. G. 1969 *J. molec. Biol.* **39**, 673.
Klug, A. & Caspar, D. L. D. 1960 *Adv. Virus Res.* **7**, 225 (especially pp. 268–270).
Klug, A., Crick, F. H. C. & Wyckoff, H. W. 1958 *Acta Crystallogr.* **11**, 199.

Note added in proof (*February* 1971)

Recent experiments show that the disk plays a key role in the assembly of the TMV particle from protein and RNA. Both nucleation and growth of the particle proceed only through the disk and the fact that it is polar is essential to the mechanisms involved (Durham, Finch & Klug, *Nature New Biol.* **229**, 37 (1971); Butler & Klug, *Nature New Biol.* **229**, 47 (1971)).

PHILOSOPHICAL TRANSACTIONS OF THE ROYAL SOCIETY B BIOLOGICAL SCIENCES

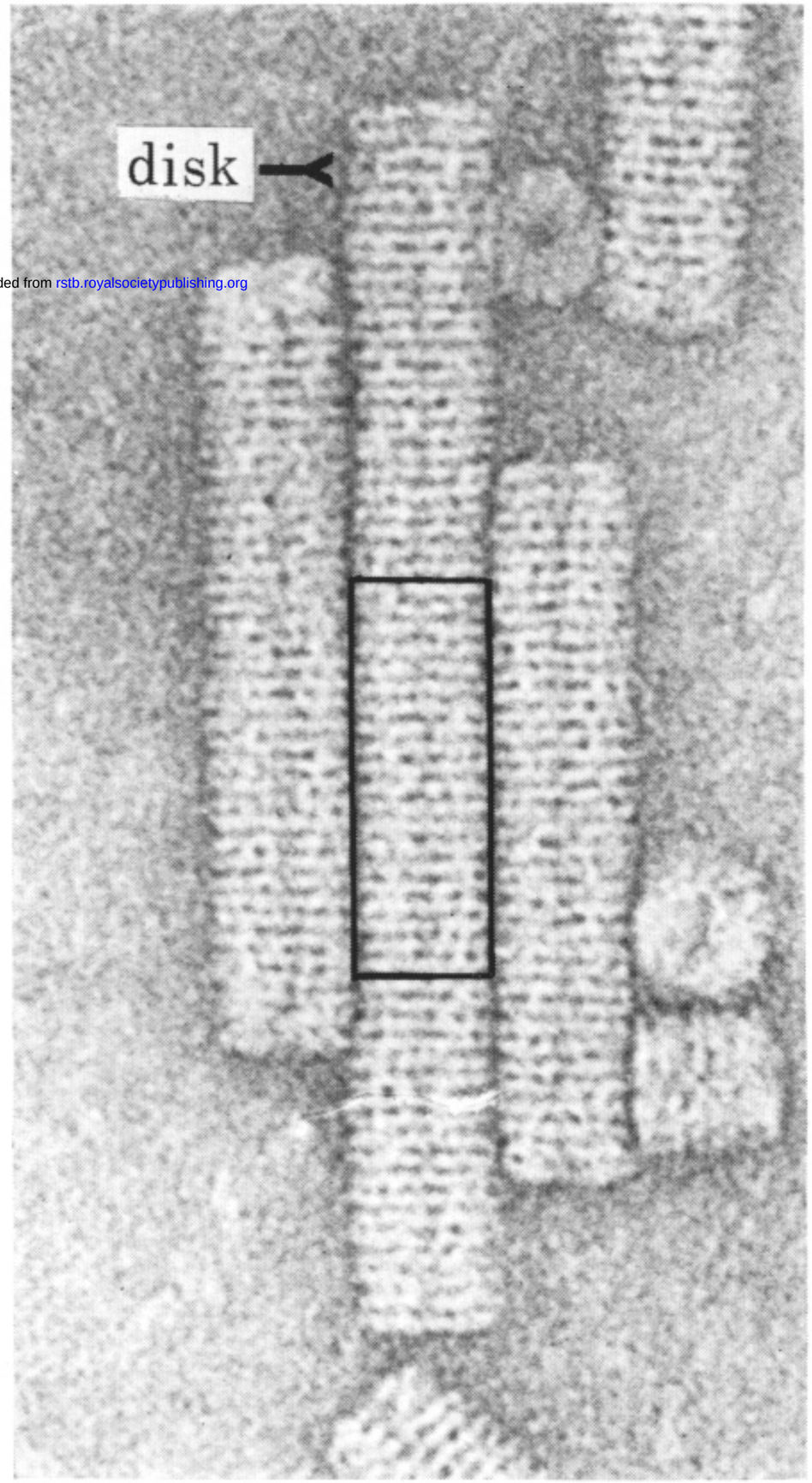

2

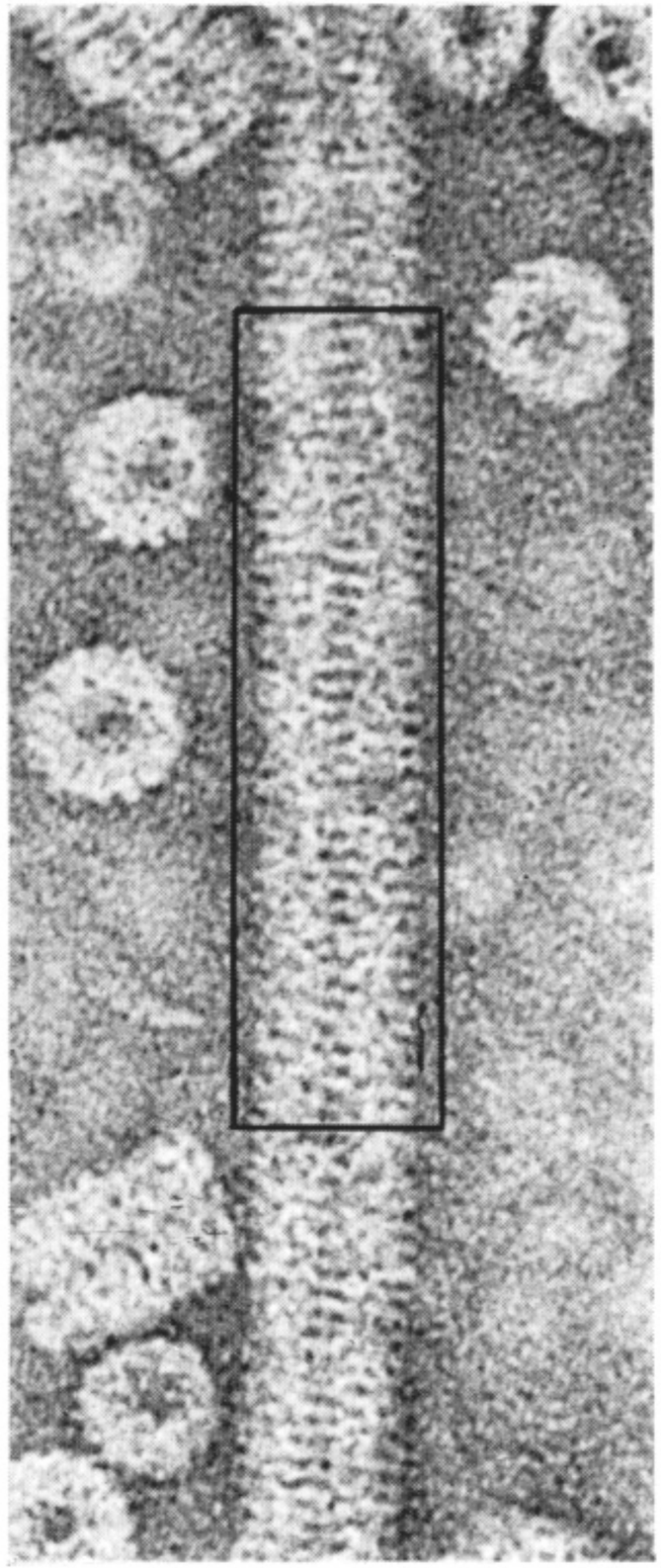

3

IGURE 2. Electron micrograph of stacked-disk rods of tobacco mosaic virus protein, negatively stained with uranyl acetate (magn. × 550 000).

IGURE 3. The double-helical aggregate of TMV protein, negatively stained with uranyl acetate (magn. × 550 000).

PHILOSOPHICAL TRANSACTIONS OF THE ROYAL SOCIETY B BIOLOGICAL SCIENCES